

## 2.8 Cryostat, Vacuum Vessel Pressure Suppression System and Thermal Shields

2.8.1	Introduction	1
2.8.2	Engineering Description	1
2.8.2.1	Cryostat	1
2.8.2.2	VVPSS	4
2.8.2.3	Thermal Shields	4
2.8.3	Performance Analysis	8
2.8.3.1	Cryostat	8
2.8.3.2	VVPSS	9
2.8.3.3	Thermal Shields	10

### 2.8.1 Introduction

The cryostat provides the vacuum environment to stop convective heat transfer to the superconducting magnets and cold structures, and forms the secondary confinement barrier for the radioactive inventory inside the vacuum vessel (VV).

The thermal shield system minimises heat loads transferred by thermal radiation and conduction from warm components to the components and structures that operate at 4.5K. Reduction of these heat loads by over two orders of magnitude is compulsory to ensure that the residual heat load at 4.5K can be removed by the ITER cryoplant with reasonable capacity.

The vacuum vessel pressure suppression system (VVPSS), which is here described in conjunction with the cryostat due to its considerable similarity to the cryostat vessel in its construction and assembly, and likelihood of procurement as part of the same package, limits the VV internal pressure, in the case of loss of coolant from the in-vessel components, to 0.2 MPa. This is a safety function as a large internal pressure could lead to a breach of the primary confinement barrier.

### 2.8.2 Engineering Description

#### 2.8.2.1 Cryostat

The design principles of the cryostat are chiefly based on cost minimisation and functionality. The cryostat is a single wall cylindrical shell with flat top and bottom. An elevation view is shown in Figure 2.8-1. Its diameter, 28 m internal, is determined by the dimension of the largest component located inside, the poloidal field coils PF4 and PF5, with an additional small radial clearance of approximately 1 m to facilitate installation of components and for access space for in-situ repair. Its height, 24 m internal, is determined by the size of components inside as well as to provide adequate vertical space for penetrations through the cryostat cylindrical shell needed to make the interconnections with external systems.

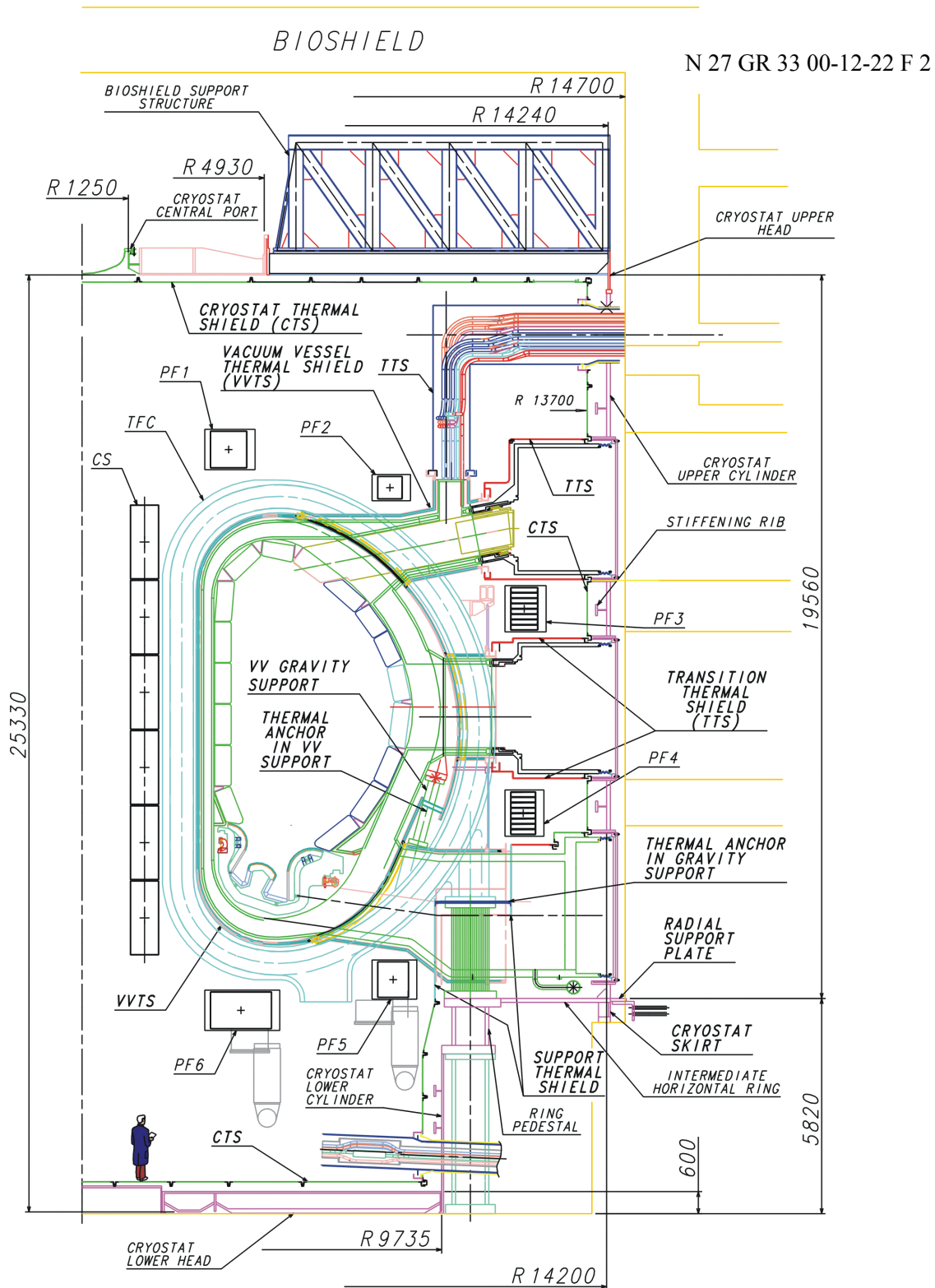


**Figure 2.8-1 Elevation View of the Cryostat and the Thermal Shield System**

The cryostat is supported by the building and surrounded by a concrete bioshield keeping a radial clearance of approximately 0.5 m. The bioshield extends above the cryostat and includes a 2 m thick slab above the cryostat that is supported by a truss structure connected to the upper head of the cryostat. The diameter of the cryostat cylinder below the VV is reduced in one step to 18 m. The reason is to facilitate a strong lateral connection between the machine supports and the building to minimise lateral movements during design basis loads including seismic events. The connection with the bioshield is at a position where an external floor slab provides additional lateral stiffness. A further feature of this design is that it improves the accessibility, through penetrations in the lower cylindrical part, into the cryostat for eventual repair or inspection access.

The cryostat is a fully-welded, stainless steel vessel with a large number of horizontal penetrations for access to VV ports at three levels and further horizontal penetrations for coolant pipework at upper and lower levels, and cryo and current feedlines to magnets at the upper and lower levels. Furthermore, access penetrations for manned or remote access for repair or inspection are included in the lower cryostat cylinder for horizontal entry and in the upper cryostat head for vertical entry. In the very unlikely case that large components located inside the cryostat need to be replaced, the upper bioshield slab can be removed, and the cryostat head with the support structure can be cut from the cryostat cylinder and also removed.

The total weight of the upper bioshield slab is approximately 3,500 t, which exceeds the capacity of the main cranes (~ 1,500 t). The bioshield slab is therefore designed to be installed and removed in several parts. The weight of the cryostat head, including the truss structure, is below 1,000 t and can therefore be removed by the main cranes without segmentation.

The upper head is a circular flat plate with radial stiffening ribs spaced every 10 degrees and integrated with the bioshield support which consists of a ferritic steel truss structure. The head, through which a neutron diagnostic penetrates, is connected via welding to the vertical cylindrical shell. The lower head is reinforced similarly to the upper head and also connected to the cylindrical shell by welding.

The main design loads considered are external pressure of 0.1 MPa, for normal operation under vacuum, and 0.2 MPa absolute internal pressure, for accidental events involving the simultaneous loss of helium and water from coolant lines routed through the cryostat. Considering the flat upper and lower ends, and particularly the large penetrations for port access, etc., through the cylindrical shell, the stability against buckling is the main driver for the mechanical design. The upper end is stabilised by the stiffening truss structure, whereas the bottom end is stabilised by ribs. The wall thickness of the cylindrical shell is generally 100 mm. Its upper, middle and lower regions are reinforced at the large divertor, equatorial and upper penetration openings. All of these shell portions are stiffened for external pressure by equally-spaced, circumferential and vertical stiffening rings and ribs. The minimum required thickness and distance between stiffening rings have been defined for external pressure in accordance with ASME code section VIII, division 2, article D-3. Because of its minimum intrusion into the inner space of the cryostat, T-section reinforcement profiles with adequate strength margin have been selected.

Large size ducts (~ 3 m H x ~ 2 m W) interconnect the VV ports with corresponding aligned penetrations in the cryostat vessel. Bellows are integrated in the duct to compensate for

differential movements. These bellows have a rectangular shape and are made of reinforced elastomer materials. Development of suitable bellows is the subject of R&D nearing completion. The results show that elastomer bellows designs with adequate pressure bearing capacity, leak tightness and radiation hardness are feasible. It is recognised, however, that outgassing rates of elastomer bellows could be higher than desirable for the operation of thermal shields etc. Hence, suitable metallic coatings or metallic bellows may have to be developed.

### 2.8.2.2 VVPSS

The VVPSS consists of a large linear tank of 46 m length and a circular cross section of 6 m diameter, containing enough room temperature water (approximately 1,200 t) to condense the steam resulting from the most adverse in-vessel coolant leak. The tank is connected to the vacuum vessel through two of the H&CD neutral beam boxes and the diagnostic neutral beam box. From these locations, three main relief pipes are routed to the VVPSS tank, each pipe incorporating double rupture disc assemblies which constitute the vacuum boundary between the vacuum vessel and the room temperature suppression water during normal operation. As described in 2.8.3.2, numerical studies predict a total relief pipe area requirement of at least 1.0 m<sup>2</sup>, in order to maintain the VV pressure below 0.2 MPa during a category IV coolant leak. In the design, this flow area is provided by two of the relief pipes, the third being redundant. The VVPSS includes a bypass system for the rupture discs, consisting of bypass pipes containing isolation valves, which are designed to open during a small coolant leak, when the vacuum vessel pressure is greater than atmospheric, but less than the opening pressure of the rupture discs. The VVPSS suppression tank is located at level + 19.7 m above the cryodistribution cold boxes in the tokamak building.

During an in-vessel coolant leak the VVPSS acts in concert with the VV drainage system, the former discharging evolved steam to the suppression tank where it is condensed, while the latter facilitates timely drainage of water from the VV to limit the amount of steam that the suppression tank has to condense. The VV drainage system is brought into play automatically by the opening of rupture discs in the VV drainage lines, for a large coolant leak, and by the opening of drainage valves for a small one. These drainage rupture discs and valves are part of the VVPSS. Additionally, the VVPSS is connected to the radioactive gaseous processing system, the low level waste processing system, the liquid and gas distribution system and the leak detection system. The VVPSS has provision to handle gaseous exhaust that could arise during a coolant leak in the VV (concurrent ingress of water, and cryogenic helium or inleakage air), by extracting such gaseous exhaust from the VVPSS tank ullage and transferring it to the standby vent detriation system (S-VDS)

Figure 2.8-2 shows a cross-section of the VVPSS tank at the location of a relief pipe connection. The VVPSS is designed for 0.2 MPa and constructed in ferritic steel. Among the load cases considered in the design is the sloshing effect of the fluid contained within the tank under seismic motion. The anchoring into the building structures is therefore an important feature of the design.

### 2.8.2.3 Thermal Shields

The thermal shields comprise the vacuum vessel thermal shield (VVTS), between the VV and the cold structures, the cryostat thermal shield (CTS), covering the walls of the cryostat (bottom, cylinder and upper head), thereby preventing direct line of sight of the room

temperature walls to the cold structures, the transition thermal shields (TTS) that enclose the port connection ducts and service lines that are routed between the cryostat walls and the VV, and the support thermal shields (STS) that enwrap the machine gravity supports. The STS also provide the thermal anchors in the VV and machine supports to reduce the conducted heat load to the cold (4.5 K) structures.

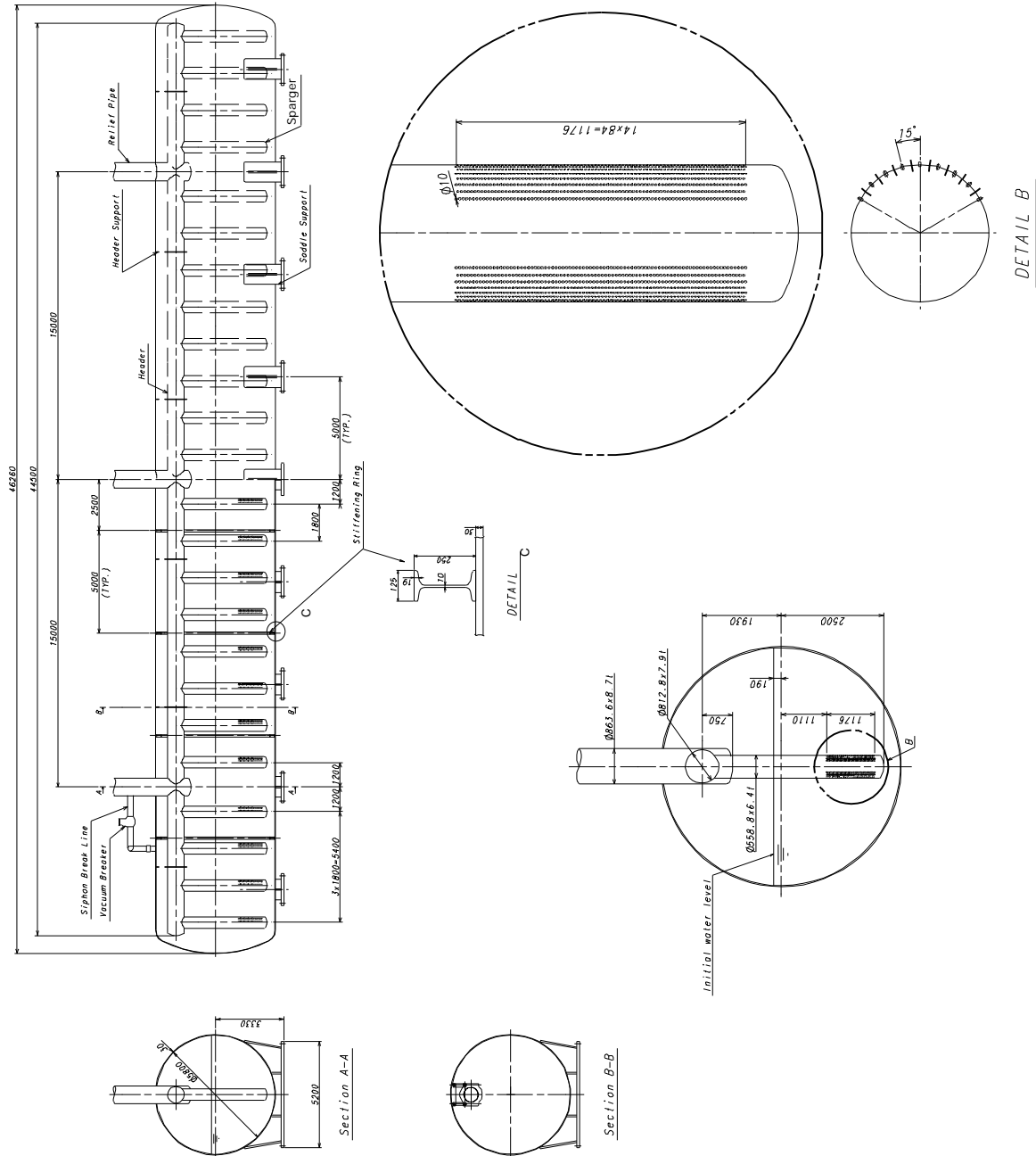


Figure 2.8-2 Vacuum Vessel Pressure Suppression Tank

A schematic elevation view of the thermal shields is shown in Figure 2.8-1. The VVTS is self-supporting under its own gravitational and thermal loads and is attached to the toroidal field coils (TFCs) by inboard and outboard supports. Inboard supports are slender Inconel rods allowing radial and toroidal movements whereas, on the outboard side, plate-type supports are used to fix the radial and toroidal position of the VVTS. All other thermal shields are modular, and fixed on the warm components via low-conductivity titanium alloy supports. Direct line of sight through the gaps between individual thermal shield plates is blocked by labyrinth-type junctions connected to the plates. The same type of labyrinth interface is used at the junctions of the different thermal shields.

In all cases the thermal shields consist of stainless steel panels that are cooled by helium gas with 80K inlet temperature. The cooling lines remove the heat load intercepted from the warm surfaces. The cold magnet structures, operating around 4K, face the TS surfaces only. The conductive heat loads from all thermal shields are merely limited to small losses through their supports. To minimise the heat load received from the warm surfaces and to reduce the heat load radiated to the 4K surfaces, the thermal shield panels are covered on both sides with a thin, low emissivity layer of silver.

While the thermal shields perform no safety function, their repair or replacement, particularly of the VVTS, would involve dismantling major parts of the VV and other in-cryostat components. Therefore, the VVTS is conservatively designed to withstand without damage all design conditions envisaged for the VV, including severe plasma disruption and seismic events, while other thermal shields have the same reliability as the in-cryostat components that surround them. Two cold valve boxes controlling the supply of helium coolant, including control valves and instrumentation, are located external to the cryostat outside the bioshield and are therefore accessible for repair or maintenance.

Furthermore, loss of cooling of the thermal shields, especially the VVTS, would lead to heating up of the cold structures. Recovery times may be very long. Therefore, the cooling system for the thermal shields is designed to be fully redundant. This not only applies to the in-cryostat cryolines, but also to the cryolines between the valve boxes and the cryoplant, as well as to the relevant cryoplant components.

To enhance the mechanical robustness, it has been decided not to employ multilayer insulation or multi-foil stacks on the thermal shields as these can be easily damaged. Moreover, the very large surface areas are difficult to outgas once contaminated by moisture and other condensables. Further enhancements against failure are obtained by having electrical breaks incorporated in VVTS panel joints, reducing the electromechanical loads on the structure and the probability of arcing between components, and by having bumpers mounted on both the inside and external side of the VVTS, thereby avoiding or mitigating impulse loads during major seismic or off-normal load events.

The space envelope is particularly critical for the VVTS. The gap between the VV and the TF coils, in which the VVTS resides, needs to be kept as small as practical. A considerable effort has therefore been expended on keeping the design of the VVTS as slim as possible. Additional clearance has to be available for thermal movements, and for the VV assembly and disassembly operations. The base design of the inboard VVTS consists of a single stainless steel panel onto which are mounted two independent helium cooling lines. The outboard part of the VVTS is made of double-wall panels for strength reasons and additionally for reducing the radiant heat loads on the magnet structures without overly

complicating the cooling tube layout, by interception of heat loads from panels facing the VV and keeping the panels facing the TF coils relatively cold (see Figure 2.8-3).

There are, in principle, two possibilities for the position of the CTS: close to the cold structures to minimise the 80K radiating area, or to connect the CTS to the cryostat wall, i.e., as far as possible away from the cold surfaces. The latter option has been selected for two reasons: (i) it allows good access to the outer perimeter of the PF and TF coils as well as to breaker boxes, clamps etc, and (ii) the overall contour of the CTS follows the cylindrical cryostat shell and is therefore much simpler for the attachment of individual panels than following the complex shape of the cold structures.

Major cost factors are the complexity of design, the high accuracy required, and the total surface area. Simplicity in design is conferred by keeping the basic panels of the CTS, TTS and STS flat and of rectangular shape for most areas. However, the VVTS has to closely follow the shape of the VV, for space reasons, and is therefore of a segmented, toroidal design. Its complexity, apart from the overall shape, lies in the fact that electrically insulated sector joints have to be made suitable for remote operations and even the initial hands-on installation is made more difficult as it is partly made through the narrow VV splice plate gaps. Figure 2.8-4 shows a 20° sector of the VVTS.

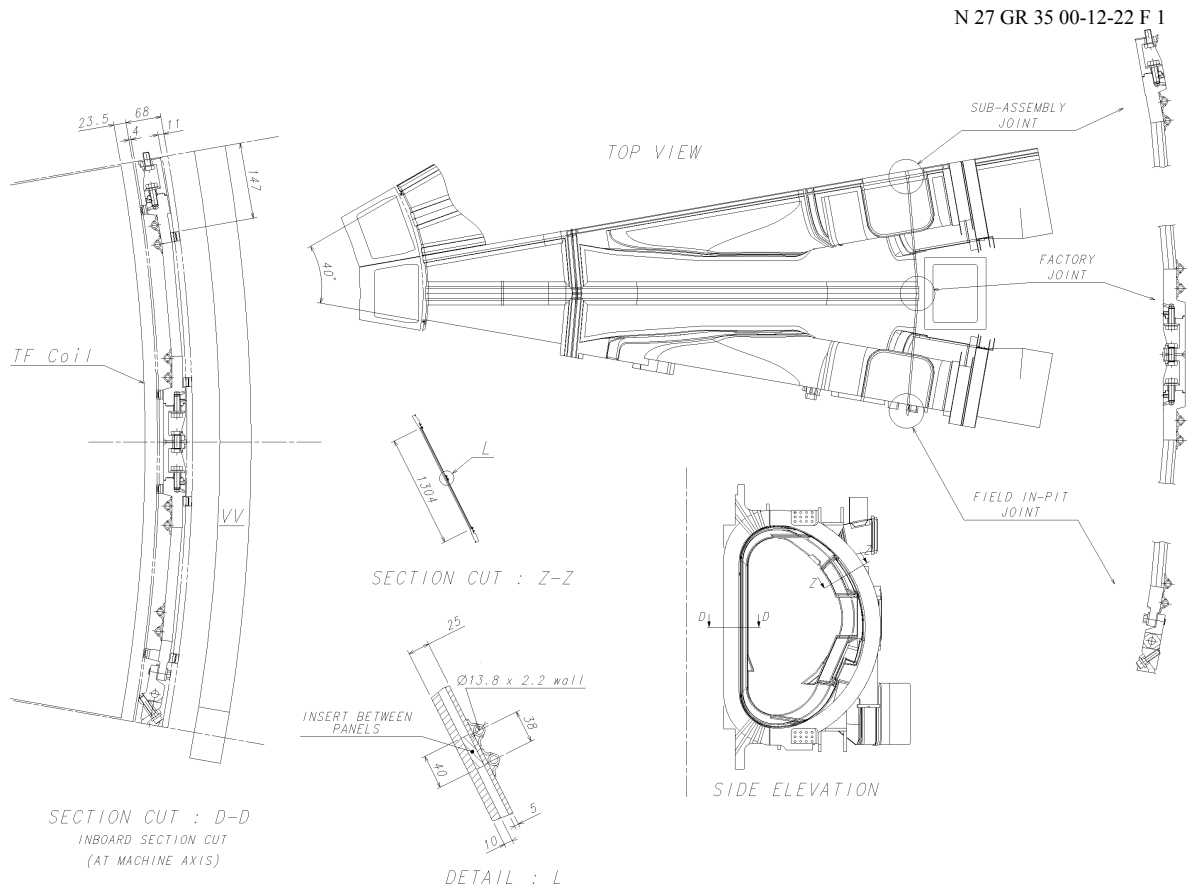


**Figure 2.8-3 VVTS Top View and Cross-section Details**

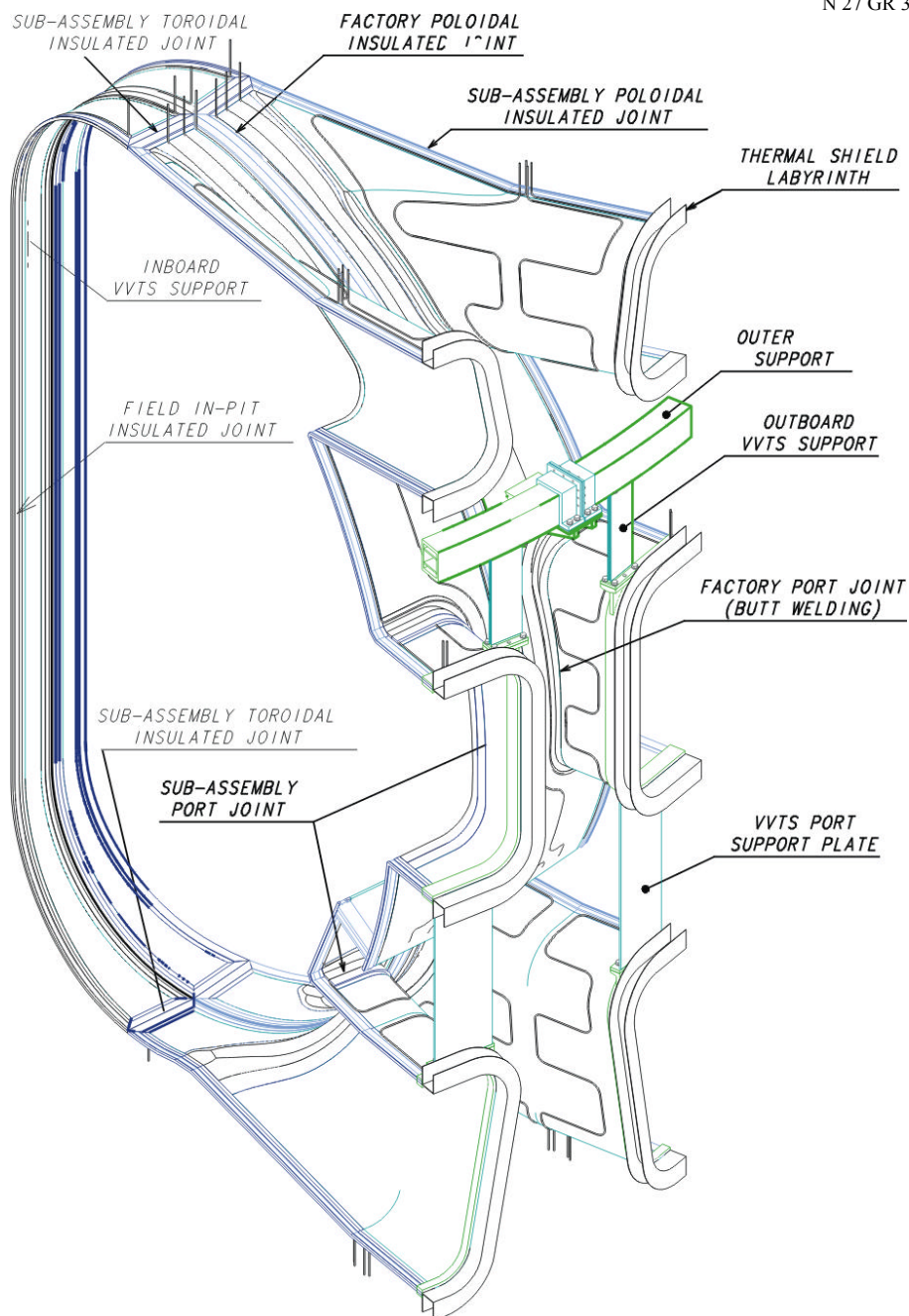


**Figure 2.8-4 Vacuum Vessel Thermal Shield 20° Sector**

## 2.8.3 Performance Analysis

### 2.8.3.1 Cryostat

The cryostat shell is subjected to loading conditions originating from various kinds of events each with its own probability. These are:

- (i) category test: dead weight + test pressure
- (ii) category I: dead weight + external pressure
- (iii) category II: dead weight + external pressure + earthquake SL-1

- (iv) category III: dead weight + external pressure + earthquake SL-2  
 (v) category IV: dead weight + helium and water ingress (internal pressure) + external pressure

Notes:

- Test pressure: The cryostat vessel is pressurised with to 0.23 MPa. absolute
- Dead weight: This loading condition arises as a consequence of gravity and the large mass of the cryostat. It is particularly significant for the top lid where a substantial amount of nuclear shielding is located.
- External pressure: This loading condition arises as a consequence of the vacuum normally present inside the cryostat. It consists of an external applied atmospheric pressure of 0.1 MPa.
- EM loads in category I: Magnet fast discharge, plasma disruption of type I, VDE of type I.
- SL-1: A seismic event of type SL-1 is classified as a likely loading condition.
- SL-2: A seismic event of type SL-2 is classified as an extremely unlikely loading condition.
- Water and helium ingress: Pressurization of the cryostat may occur as a consequence of helium expelled from the magnet into the cryostat simultaneously with hot water.

A finite element model is employed for the analysis of the cryostat vessel. Given the different layout of the smaller openings in different machine sectors, the worst location has been used for modelling, and symmetry boundary conditions have been employed. The analysis model consists of shell elements and beam elements. The analysis for category-test and category I has been performed for the upper cylinder with a model of 10°, which is a half of one cylinder sector. The cylinder and port flanges are modelled with shell elements and stiffening ribs are modelled with beam elements. All stress levels at notable locations are within the allowable stresses. A detailed analysis using a 180° model including other parts of the cryostat is in progress.

### 2.8.3.2 VVPSS

The bases of the required total flow area of the relief pipes and the quantity of suppression water are results obtained from numerical studies using the MELCOR code.

On the basis of the MELCOR code study, the total relief pipe flow area has to be at least 1.0 m<sup>2</sup>. Additionally the code results predict that a drain line flow area of at least 0.1 m<sup>2</sup> is required to drain residual water rapidly enough to keep the final suppression water temperature to the design limit.

The pressure in the VV peaks at 0.17 MPa 10 s after the start of the coolant leak.

The suppression tank is required to have an interior volume of at least 1,200 m<sup>3</sup>. A low pressure is maintained inside (0.23 kPa). The tank contains 650 m<sup>3</sup> of suppression water, which is needed to condense the steam arising from an in-vessel coolant leak while subcooled until the end of the event. The tank is subject to loading conditions originating from various kinds of events. A set of loading combinations has been established for evaluation of the VVPSS structure:

- (i) category test: dead weight + test pressure
- (ii) category I: dead weight + external pressure
- (iii) category II: dead weight + external pressure + water head + internal pressure

(small coolant leak)

(iv) category III: dead weight + external pressure + water head + earthquake SL-1

(v) category IV: dead weight + external pressure + water head + earthquake SL-2

(vi) category IV: dead weight + external pressure + water head + internal pressure

(large coolant leak)

Notes:

- Test pressure: The tank is pressurized to 0.23 MPa absolute to verify its structural integrity after construction.
- Dead weight: This loading conditions arises as a consequence of gravity and the structural mass of the tank.
- Water head: The lower half of the tank volume contains water during normal operating conditions.
- External Pressure: This loading condition arises as a consequence of the near vacuum conditions normally present inside the tank. It consists of an external applied atmospheric pressure of 0.1 MPa.
- Small coolant leak: The steam pressure in the VV will trigger the active opening of bleed lines which will connect the VV to the tank. The peak pressure is less than 0.1 MPa.
- Large coolant leak: The steam pressure in the VV will trigger the passive opening of rupture disks which will connect the VV to the tank. The peak pressure is less than 0.2 MPa.

For protection against buckling due to external pressure, stiffening ribs are welded to the inside surface of the tank at longitudinally equal pitches, in accordance with the requirement of ASME code section VIII, division 2, article D-3.

### 2.8.3.3 Thermal Shields

The thermal shield system is subjected to a large spectrum of loading conditions and combinations thereof. The main loads are gravity, seismic, electromagnetic and thermal gradients.

#### *Thermal loads*

Detailed analysis of the thermal loads is very important for ensuring that the thermal shields can handle the loads both locally, without excessive stress and thermal traction, and globally to interface with the cryoplant within the specified boundary conditions, and in particular, to ensure that the cryoplant can handle the heat loads in a cost-effective manner. The main results of thermal load analysis for both the plasma operation state (POS) and VV baking state (BOS), together with the associated thermal shield thermohydraulic data, are summarised in Table 2.8-1. Pressured helium gas from the main cryogenic plant, with an inlet temperature and pressure of 80K and 1.8 MPa respectively, is used to cool the thermal shield system. The total helium mass flow rate for all thermal shields is 4.5 kg/s.

The total pressure drops are 88 and 89 kPa for POS and BOS respectively. The total heat loads on the magnet system are about 10 kW and the total pressure drop is less than the cryoplant interface limit of 100 kPa. There is potential for a significant reduction in heat load from the labyrinths by further optimising the geometry and surface emissivity. To implement this optimisation, additional refined thermal analysis is required.

**Table 2.8-1 Thermal Shield Thermohydraulic Data and Results of Thermal Analysis**

	VVTS	CTS and STS	TTS	VV Thermal Anchors (TAs)	TAs in Machine Gravity Supports
Surface area, m <sup>2</sup>	2,430	2,400	2,330	-	
Total mass, t	476	280	260	-	25.1
Inner tube diameter, mm	9.5	22.9	22.9	10	7.7
Maximum tube length, m	21	160	110	13.1	4
Inner manifold diameter, mm	70	82.5, 107	54.3,	54.3	54.3
Maximum manifold length, m	206	188	216	206	216
Max. outlet He temperature, K:					
POS	100	95	95	100	85
BOS	121	95	119	110	85
Mass flow rate, kg/s	1.87	0.90	2.36	0.2	0.73
Heat loads to shield coolant*, kW:					
POS	194	70	184	19	19
BOS	392	94	386	23	19
Heat loads to cold mass (POS), kW					
radiation from surface	0.70	0.55	0.95	-	-
radiation from labyrinths	1.55 <sup>(1)</sup>	1.8 <sup>(2)</sup>	0.5 <sup>(3)</sup>	-	-
conductance through supports	0.1	-	-	1.7	2.3
Maximum panel temperature rise, K:					
POS	19/53 <sup>(4)</sup>	10	36	-	10
BOS	32/87 <sup>(4)</sup>	10	60	-	10

\*Radiation on surface and captured in labyrinth, nuclear heating and conductance

<sup>(1)</sup> VVTS/TTS, VVTS/STS labyrinths; <sup>(2)</sup> CTS/TTS, CTS panels, CTS/STS labyrinths;

<sup>(3)</sup> STS/TTS, TTS panels labyrinth; <sup>(4)</sup> Values for single and double plate parts of the VVTS respectively.

The heat loads to cold mass (radiation from surface and labyrinths, and conductance through supports) are somewhat higher than those quoted in Table 2.1.1-4 based on earlier estimates. Design modifications are being studied to reduce these loads.

### *Structural analysis*

Hoop stresses induced by the coolant pressure load are very modest. The 1.8 MPa helium in the largest tubes, 23 mm ID with 2 mm walls, gives a hoop stress of only 11 MPa, and in the largest manifold is 27 MPa. Stresses in tube bends and connections are well within allowable values.

Gravity loading is not critical for the thermal shields. The maximum deflection of the VVTS and TTS/CTS panel under gravity loading is less than 2.5 mm and the stress level is within the allowable.

Eddy currents induced in the thermal shields during disruption and fast discharge cross magnetic fields and produce electromagnetic (EM) loads. Electrical breaks in the poloidal and toroidal direction for the VVTS, and judicious selection of the CTS and TTS panel

dimensions, is required to mitigate these loads. Detailed finite element static EM analyses and stress analysis for the most adverse design regimes have been performed for the VVTS sector. The main results are presented in Table 2.8-2, and indicate that 36 toroidal and two poloidal breaks are sufficient from the standpoint of limiting stresses and deflections to acceptable values.

**Table 2.8-2 Main Results of VVTS Stress Analysis under Dead Weight, EM Loads and TFC Out-Of-Plane Deformation**

<b>Regime</b>	<b>Max, Displacement,mm</b>	<b>VVTS Shell/Flange <math>P_L+P_b^*</math>,MPa</b>	<b>Inboard Support <math>P_m^*</math>,MPa</b>	<b>Outboard Support <math>P_L+P_b^*</math>,MPa</b>	<b>Port Support Plate <math>P_L+P_b^*</math>,MPa</b>
Dead weight (DW)	2.5	21/78	181	38	4.2
Plasma Disruption Types I&II + DW	2.4	23/25	186	151	16
Types III Fast VDE + DW	2.8	40	192	145	26
Types III Slow VDE + DW	3.9	35/135	192	145	36
TFC Fast Discharge + DW	1.5	17	178	30	14
		$P_L+P_b+Q^*$ , MPa	$P_L+P_b+Q^*$ , MPa	$P_L+P_b+Q^*$ , MPa	
TFC Out-plane Deformation +DW	19	84	138	69	

\* $P_m$  – general membrane stress,  $P_L+P_b$  – local membrane plus bending stress,  $P_L+P_b+Q$  – primary plus secondary stress.

The design of the TTS panel has been driven by the large EM loads caused by a central plasma disruption with and without simultaneous PF fast discharge. The maximum deflection is 2.6 mm and the  $P_{m+L}$  value does not exceed 190 MPa, confirming that the design of the panel is adequate. The analysis of the TTS and STS panels under EM loads during other design regimes is in progress.

The out-of-plane deflection of the TF coils (17.3 mm during each pulse) results in a bending deformation of outer supports and rotation of the whole VVTS. The stresses in the VVTS for such condition (summarised in Table 2.8-3) are within the acceptable limits for static and cyclic loads.

Both detailed and global FE thermal and mechanical analysis shows that temperature gradients between the coolant tube and panels, caused by the high radiant heat flux (Figure 2.8-5), lead to considerable local stress. However, the stress is less than the  $3S_m$  limit for the VVTS and for the CTS/TTS panels for both POS and BOS regimes. Thermal stress for the two-layer outboard VVTS remains to be checked. The stress level in the titanium alloy support, due to temperature differences between warm components and the TS panel, reaches 500 MPa, but is still within the allowable range.

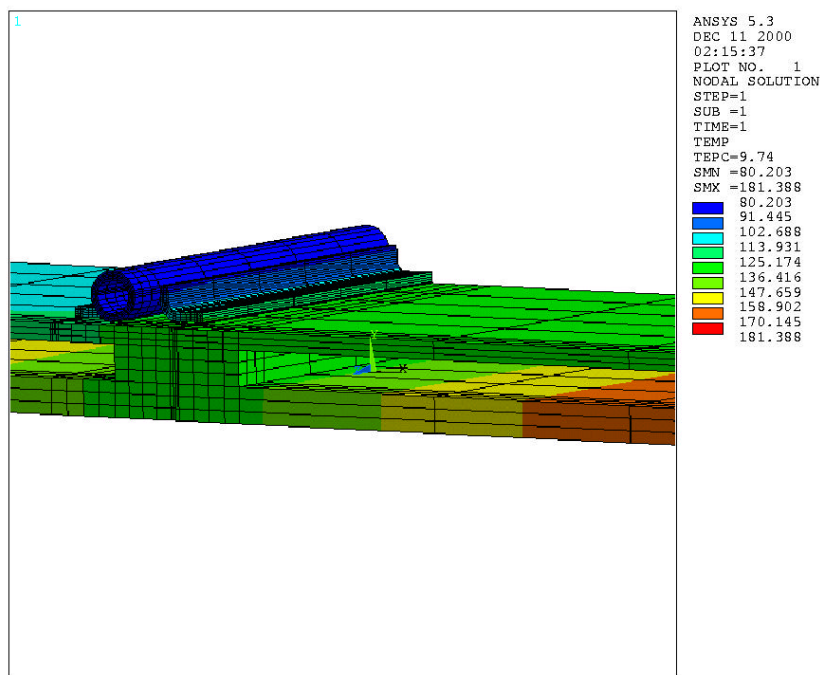


**Figure 2.8-5 Temperature in VVTS Outboard Panel (K) at VV Baking,  $T_{He} = 80K$   
 - Detailed View**

### *Seismic analysis*

The results of a seismic analysis of the whole tokamak, which included a model of the VVTS, are presented in Table 2.8-3. After modification of the VVTS support design, the relative displacements between the VV and the VVTS as well as the TFC and the VVTS are quite small and the existing available gaps can accommodate them.

**Table 2.8-3 Mutual Seismic Displacements between VVTS and Adjacent Components  
 (SL-2: Ground Acceleration of 0.2 g)**

Name	Radial, mm		Toroidal, mm		Vertical, mm	
	TS/TFC	TS/VV	TS/TFC	TS/VV	TS/TFC	TS/VV
Equatorial inboard	6.6	1.8	6.6	1.8	1.1	2.8
Top	4.4	3.6	4.2	3.4	2.5	2.9
Bottom	8.6	3.2	8.9	3.3	2.0	3.0
Upper port upper outer corner		3.3		4.0		2.9
Lower port lower outer corner		3.2		3.3		2.7
Lower port lower inner corner		3.0		3.6		3.5

As the theoretical contact between TFC and VVTS is restricted to the bumpers at the inboard and bottom part, it is foreseen that no damage of the VVTS panels will occur during a seismic event. Equivalent static analyses of the CTS and TTS panels have been performed,

under an acceleration of 0.8 g and 1.2 g respectively. These seismic loads are considerably less than the EM loads, and does not give problems with stress and deflection in the panels and their supports.

One remaining issue is the upward force in the inboard support, which can lead to increased tensile force during the subsequent downward motion. Further optimisation of the VVTS support structure is in progress.

Seismic analysis of the whole tokamak including cryostat, VV port connecting ducts and a refined VVTS model is important for confirmation of the results presented herein, determination of mutual displacements in other critical regions, and the acceleration of the CTS and TTS support structures.

#### *Fatigue analysis*

A detailed analysis of the fatigue lifetime of the TS under thermal loads has been performed. Even when applying very conservative assumptions, there appears to be no fatigue problems with TS components. However, more detailed fatigue analysis is still required, and planned for the near future, for bolts and dowel pins.

#### *Buckling analysis*

A selective buckling analysis has been performed for the VVTS under dead-weight and most critical EM loads. The safety factor for buckling is higher than 10, which is adequate. Additional analysis has revealed adequate buckling margin for the CTS/TTS panel supports.

#### *Dynamic analysis*

Modal analysis of the VVTS and TS panel has shown that EM loads can lead to significant dynamic effects, and therefore a dynamic analysis of the TS is planned. Meanwhile, a dynamic coefficient of 2 has been applied to the results of static stress analysis and a peaking factor of 1.3 for VDE regimes. The obtained stress levels and deflections are still very moderate.

#### *Gap analysis*

At the inboard, where the space is at premium, the gap between TFC, VVTS and VV has to be minimised. The gap analysis had to account for fabrication and installation tolerances, required assembly clearances, mutual seismic and thermal movements, which reach 85 mm in some regions, as well as deflection under all design loads. The allocated clearance between TFC and VV is 144 mm, which allows a 30 mm gap for the insertion of a backside protection during the cutting of a VV sector. In order to meet these requirements, the VVTS inboard part has been redesigned and the assembly procedures have been checked with 3D CATIA CAD analysis of the clearances.

#### *Thermal shield baking*

Thermal shield baking is very important for conditioning the TS surface and attaining good cryostat vacuum quality. Thermal shield baking is presently being studied, together with related vacuum quality aspects, with a view to specifying a limit for cryodeposition of

condensable gases on the thermal shields during cool-down, which could cause the degradation of the reflective surfaces. Active warm-up of the CTS with acceptable pressure drop requires operation of both active and redundant loops, and additional heaters and coolers of significant size. A temperature of above 110°C can be achieved by passive radiant heating of the VVTS and TTS from the baked VV at 200°C and by simultaneous active warm-up of CTS by pressured He from the cryoplant.